Direct Numerical Simulation of Channel Flow with Transpired Wall

Y. Na [1]
1. Multidisciplinary Aerospace System Design Team,
Department of Mechanical Engineering, Konkuk University,
Kwangjin-gu, Hwayang-dong, 1, Seoul 143-701, Korea, yangna@konkuk.ac.kr

Corresponding author ***Y. Na***

Abstract

The present work investigates turbulent velocity and temperature fields subject to strong wall injection in a channel using a Direct Numerical Simulation technique. A simplified model problem of the internal flows inside the hybrid rocket motors where a regression process at the wall is idealized by the wall blowing has been considered to gain a better understanding of how the turbulent structures are modified. Since the near-wall state of turbulence is likely to be modified due to the effect of wall blowing and the mean flow dynamics differ significantly from those in typical non-transpired channel flows, caution needs to be made when the RANS type calculations are to be performed. As the strength of wall blowing increases, the flow experiences stronger streamwsie acceleration or inhomogeneity and both the wall shear and friction temperature decrease significantly but many of higher order statistics such as turbulence intensities, turbulent heat flux, r.m.s. temperature fluctuations and Reynolds shear stress increase rapidly as the flow moves downstream and this is thought to result from the shear instability induced by wall injection. Also, turbulent viscosity and turbulent diffusivity grow rapidly. Thus, the effect of wall-blowing modifies the state of turbulence significantly and more sophisticated turbulence modeling is required to predict this type of flows accurately.

Keyword: *Turbulent Flow, Wall Injection, Direct Numerical Simulation, Passive scalar, Turbulent Prandtl number*

1. Introduction

Turbulence plays an important role in the mean flow dynamics and turbulence quantities in hybrid rocket motors. In addition to the usual effect of turbulence on the flow, turbulence interacts with combustion process through turbulent fluctuations and would influence the dispersion of boron or aluminum dioxide. Since the near-wall state of turbulence is likely to be modified due to the effect of wall blowing, caution needs to be made when the RANS type calculations are to be performed.

Better understanding of injection driven flows such as those present in hybrid rocket motors would require the high quality data on the statistics and turbulence mechanisms but there has been significantly less effort both in experimental and turbulence modeling studies than in other common shear flows. Most of previous studies (Beddini [1]; Traineau et al. [2]; Dunlap et al. [3]; Liou and Lien [4]) devoted to the analysis of wall-bounded flows with wall injection have dealt with very weak blowing or laminar flow. The present work is motivated by the need for the data of turbulent flow and temperature field in the presence of strong wall-injection to understand the evolution of the flow and physical process in near-wall region and to support the RANS and LES modeling developments. A method of direct numerical simulation is used to obtain detailed flow field information on velocity and temperature (assumed as a passive scalar) fields. In order to see the effect of wall blowing, the mean flow and turbulence statistics which differ significantly from those in typical non-transpired channel flow will be mainly discussed.

Report Documentation Page

Form Approved
OMB No. 0704-0188

1. REPORT DATE **14 APR 2005**	2. REPORT TYPE **N/A**	3. DATES COVERED **-**

4. TITLE AND SUBTITLE **Direct Numerical Simulation of Channel Flow with Transpired Wall**	5a. CONTRACT NUMBER 5b. GRANT NUMBER 5c. PROGRAM ELEMENT NUMBER
6. AUTHOR(S)	5d. PROJECT NUMBER 5e. TASK NUMBER 5f. WORK UNIT NUMBER
7. PERFORMING ORGANIZATION NAME(S) AND ADDRESS(ES) **Multidisciplinary Aerospace System Design Team, Department of Mechanical Engineering, Konkuk University, Kwangjin-gu, Hwayang-dong, 1, Seoul 143-701, Korea**	8. PERFORMING ORGANIZATION REPORT NUMBER
9. SPONSORING/MONITORING AGENCY NAME(S) AND ADDRESS(ES)	10. SPONSOR/MONITOR'S ACRONYM(S) 11. SPONSOR/MONITOR'S REPORT NUMBER(S)

12. DISTRIBUTION/AVAILABILITY STATEMENT
Approved for public release, distribution unlimited

13. SUPPLEMENTARY NOTES
See also ADM001800, Asian Computational Fluid Dynamics Conference (5th) Held in Busan, Korea on October 27-30, 2003. , The original document contains color images.

14. ABSTRACT

15. SUBJECT TERMS

16. SECURITY CLASSIFICATION OF:			17. LIMITATION OF ABSTRACT	18. NUMBER OF PAGES	19a. NAME OF RESPONSIBLE PERSON
a. REPORT **unclassified**	b. ABSTRACT **unclassified**	c. THIS PAGE **unclassified**	**UU**	**6**	

Standard Form 298 (Rev. 8-98)
Prescribed by ANSI Std Z39-18

2. Numerical details

2.1 Governing equations

A simplified yet sufficiently realistic model problem has been considered to enable DNS. Also Reynolds number is set low so that DNS is tractable and still reasonably captures the flow characteristics. The flow configuration presented in Fig. 1 shows that the regression process at the propellant surface is idealized by the wall injection. The streamwise extent of the domain is L_x=26h, the spanwise extent is L_z=6.5h where h is the half channel height. In terms of wall units (based the friction velocity at inlet of the domain), the domain size is roughly equivalent to 3820, 294, 955 in the streamwise, wall-normal and spanwise directions, respectively and a length of about 1900 wall units is allowed for the injection-driven flow regime.

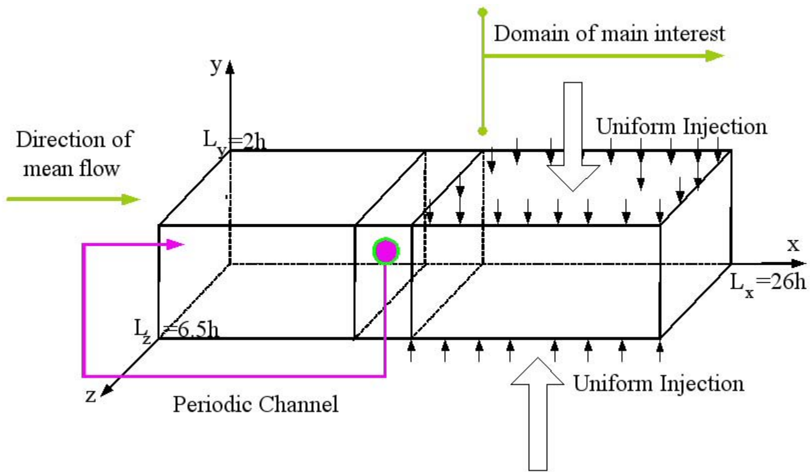

Fig. 1. Flow configuration

Since the Mach number in the hybrid motor is in general less than 0.1, the following non-dimensionalized governing equations for velocity and temperature fields of unsteady incompressible viscous flows are solved on a rectangular staggered grid (Harlow and Welch [5])

$$\frac{\partial u_i}{\partial x_i} = 0 \tag{1}$$

$$\frac{\partial u_i}{\partial t} + \frac{\partial (u_i u_j)}{\partial x_j} = -\frac{\partial p}{\partial x_i} + \frac{1}{\mathrm{Re}_h}\frac{\partial^2 u_i}{\partial x_j^2} \tag{2}$$

$$\frac{\partial T}{\partial t} + \frac{\partial (T u_j)}{\partial x_j} = \frac{1}{\mathrm{Re}_h \Pr}\frac{\partial^2 T}{\partial x_j^2} \tag{3}$$

All the variables are made dimensionless using an inlet bulk velocity, upper wall temperature and a half-channel height. It is assumed that the fluid density is independent of temperature so that the heat is essentially transported as a passive scalar, without producing buoyant force.

The governing equations (1)-(3) are integrated in time using a semi-implicit scheme. A low-storage three-substep, third order Runge-Kutta scheme (Spalart et al. [6]) is used for treating convective terms explicitly and a second order Crank-Nicolson scheme is used for treating viscous terms semi-implicitly. All spatial derivatives are approximated with second order central difference scheme except for the convection term in equation (3). It has been reported that the central differencing applied to convection terms in the passive-scalar equation with inflow-outflow boundary condition leads to numerical instability (Akselvoll and Moin [7]) and thus, widely used QUICK scheme (Leonard [8]) was incorporated as a remedy for the present work.

2.2 Boundary conditions

The no-slip boundary is used along the wall except in a region where constant blowing is set up to be applied (x/h>13.4). The bottom wall is cooled and the top wall is assumed to be heated at the same rate so that both walls are maintained at constant temperature and respectively). The flow is assumed to be homogeneous in the spanwise direction.

A popular convective boundary condition was used for the outflow boundary condition and in order to generate a turbulent inlet condition as a function of time, a periodic channel is attached in front of the domain of main interest where the injection is applied.

2.3 Calculation of statistical quantities

The Reynolds number, Re_h is set to 2250 and it is approximately equivalent to 150 when the inlet friction velocity is used. The Prandtl number was set to 1. Computations were conducted with two different resolutions (257x129x129 and 513x257x129) in order to see the effect of resolution on the results but only the results with higher resolution (513x257x129) will be presented here otherwise indicated. This grid system gives the resolution of approximately $\Delta x^+ \approx 7.5$, $\Delta y^+_{\min} \approx 0.0055$, $\Delta y^+_{\max} \approx 1.8$, $\Delta z^+ \approx 7.5$ using wall variables defined at inlet of the domain. The effect of resolution was checked with previous channel flow results obtained with pseudo-spectral method (Na et al. [9]).

For the calculation of statistical quantities, averages were performed over the homogeneous spanwise direction and time and hence, single-point statistics are functions of both x and y. In the present flow configuration, the flow experiences complex changes after the injection is applied and this causes slower statistical convergence than in the upstream. The total averaging time was 60.

3. Results

Due to the strong wall injection, the flow experiences strong acceleration or inhomogeneity as the flow goes through a region of wall injection. Also, the hydrodynamic and thermal boundary layers are totally displaced away from the wall, which in turn results in low skin friction and friction temperature. Figs. 2-3 show the mean streamwise velocity and temperature profiles at several streamwise locations.

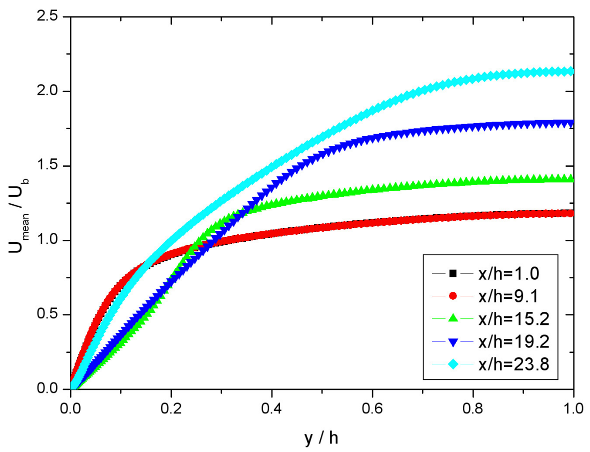

Fig. 2. Profiles of mean streamwise velocity

The progression of mean streamwise velocity and temperature profiles suggest that they deviate significantly from that of non-transpired channel flow. Since the boundary layers are displaced from the wall, the velocity gradient and temperature gradient at the wall drop significantly.

Other second order statistics including u_{rms} and T_{rms} also increase as the flow goes through a region of higher pressure gradient induced by the wall injection and are skewed to the middle of the channel.

Figs 4-5 show the following mean temperature equation budget at two representative locations, x/h=19.2 and x/h=23.8.

$$0 = -\left\{ \frac{\partial(\overline{T}\overline{u})}{\partial x} + \frac{\partial(\overline{T}\overline{v})}{\partial y} \right\} + \frac{1}{\mathrm{Re}_h \Pr} \left(\frac{\partial^2 \overline{T}}{\partial x^2} + \frac{\partial^2 \overline{T}}{\partial y^2} \right) - \left\{ \frac{\partial \overline{T'u'}}{\partial x} + \frac{\partial \overline{T'v'}}{\partial y} \right\} \tag{4}$$

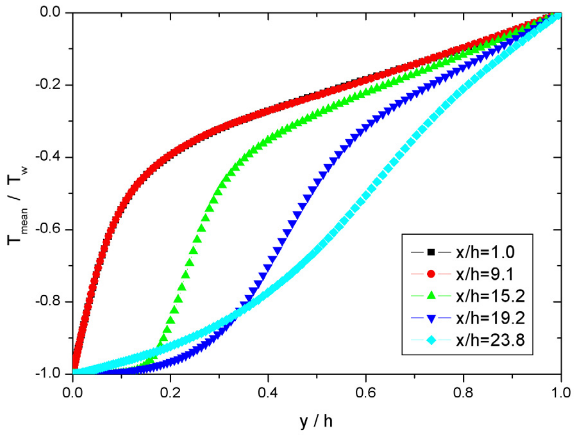

Fig. 3. Profiles of mean temperature

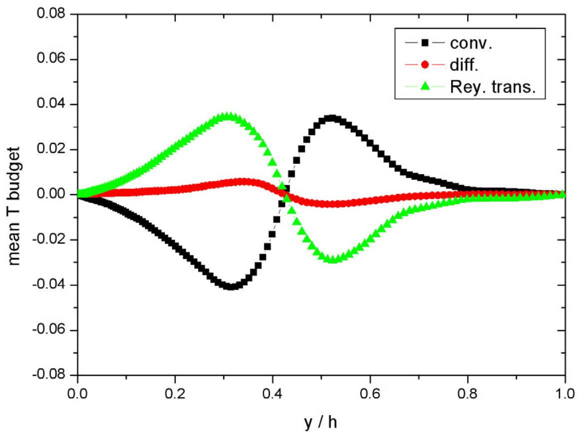

Fig. 4. Mean temperature equation budget at x/h=19.2

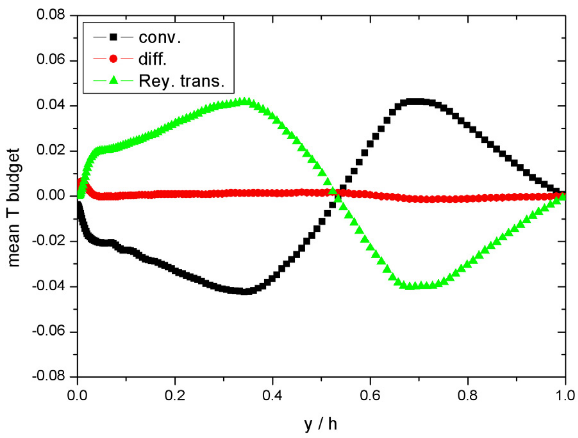

Fig. 5. Mean temperature equation budget at x/h=23.8

For non-transpired wall, the Reynolds heat flux and viscous terms are dominant and usually the variation of terms in the streamwise direction is negligible compared to that in the wall normal direction. But Figs. 4-5 clearly reveal that the convection term is one of the major terms in the budget. This result is different from that of mean momentum equation budget in that the pressure gradient term is dominant in the mean streamwise velocity equation budget.

A bulwark of $k-\varepsilon$ and Reynolds stress closure models is the definition of a characteristics time scale. In the conventional $k-\varepsilon$ model, the turbulent viscosity is taken as $\nu_t \sim k\tau \sim k^2/\varepsilon$. Similarly, in an attempt to model α_t, different time scale τ_T which is defined as $\alpha_t \sim k\tau_T$ has been suggested. The variation of temperature dissipation or time-scale is found to show strong variation in the streamwise direction. This indicates that the prediction of passive scalar field will not be easy because its accuracy strongly depends on the quality of the RANS modeling. Thus, a critical test for the models of scalar transport will be their ability to predict the influence of wall injection on various temperature statistics.

Finally, the turbulent Prandtl number profiles are shown in Fig. 6. Strong variation with x in the near wall region is noted. It shows that an initiation of strong wall injection results in a sharp drop of turbulent Prandtl number. As the flow goes through a region of strong pressure gradient, the turbulent Prandtl number recovers slowly. Thus, a rapid change of turbulent Prandtl number suggests that the modeling for velocity and temperature field can not be done in a same way.

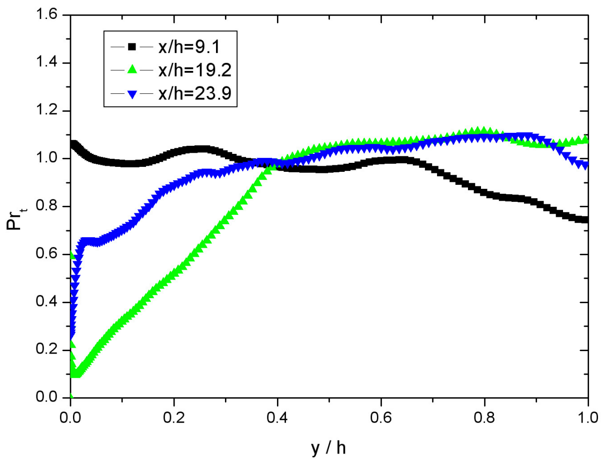

Fig. 6. Profiles of turbulent Prandtl number

4. Summary

The effect of strong wall-injection on velocity and temperature field has been investigated using a DNS technique in the model injection-driven internal flow and various statistical quantities were reported. The complexity of the flow comes from the interaction of the mean flow with strongly injected normal flow at the wall and the subsequent evolution of the flow is characterized by a non-negligible streamwise inhomogeneity.

Many of turbulent statistics such as turbulence intensity, Reynolds stress and Reynolds heat flux show a rapid increase in a region of strong wall injection and the velocity and temperature fields respond to the wall injection to a different degree. This behavior will raise an issue that low heat transfer rate near the propellant surface influences the regression process in an adverse manner.

Mean temperature equation budget shows that the Reynolds heat flux terms are important as opposed to that in mean momentum equation budget and thus, the conjecture that the prediction of the mean flow alone will not be very sensitive regardless of turbulence models used does not hold.

The classical approach in turbulent scalar transport study is to use the analogy which assumes that the turbulent diffusivity is proportional to the turbulent viscosity. But the present result indicates that the turbulent Prandtl number shows large variation in the strong-injection driven flow and this will add the difficulty to the turbulence modeling work.

,

References

[1] Beddini, R. A., "Injection-Induced Flows in Porous Walled Ducts," *AIAA J.* , Vol. 24, No. 11, (1986), pp. 1766～1773.

[2] Traineau, J. -C., Hervat, P. and Kuentzmann, P., "Cold Flow Simulations of a Two Dimensional Nozzleless Rocket Motor," Tech. Rep. 86-1447. AIAA, (1986).

[3] Dunlap, R., Blackner, A. M., Waugh, R. C. Brown, R. S. and Willoughby, P. G, "Internal Flow Field Studies in a Simulated Cylindrical Port Rocket Chamber," *J. Prop. Power*, Vol. 6, No. 6, (1990), pp. 690～704.

[4] Liou, T. M. and Lien, W. Y., "Numerical Simulations of Injection-Driven Flows in a Two Dimensional Nozzleless Solid Rocket Motor, " *J. Prop. Power*, Vol. 11, No. 4, (1995), pp. 600～606.

[5] Harlow, F. H. and Welch, J. E., "Numerical Calculation of Time Dependent Viscous Incompressible Flow of Fluid with Free Surface," *Phys. Fluids,* Vol. 8, (1965), pp. 2182～2189.

[6] Spalart, P. R., Moser, R. D. and Rogers, M., "Spectral Methods for the Navier-Stokes Equations with One Infinite and Two Periodic Directions," *J. Comput. Phys*., Vol. 96, (1991), pp. 297～324.

[7] Akselvoll, K. & Moin, P., "Large Eddy Simulation of Turbulent Confined Coannular Jets and Turbulent Flow Over a Backward Facing Step", Rep. TF-63, Thermoscience Division, Dept. of Mechanical Eng., Stanford University, (1996).

[8] Leonard, B. P., “A Stable and Accurate Convective Modeling Procedure Based on Quadratic Upstream Interpolation", *Comput. Methods Appl. Mech. Eng.*, Vol. 19, (1979), pp. 59.

[9] Na, Y., Papavassiliou, D. V. and Hanratty, T., "Use of Direct Numerical Simulation to Study the Effect of Prandtl Number on Temperature Fields," *Int. J. Heat and Fluid Flow*, Vol. 20, (1999), pp. 187～195.